IOP Conf. Series: Materials Science and Engineering **192** (2017) 012007 doi:10.1088/1757-899X/192/1/012007

On the theory of ternary melt crystallization with a non-linear phase diagram

L V Toropova, G Yu Dubovoi and D V Alexandrov

Department of Theoretical and Mathematical Physics, Laboratory of Multi-Scale Mathematical Modeling, Ural Federal University, Ekaterinburg, 620000, Russian Federation

E-mail: l.v.toropova@urfu.ru

Abstract. The present study is concerned with a theoretical analysis of unidirectional solidification process of ternary melts in the presence of a phase transition (mushy) layer. A new analytical solution of heat and mass transfer equations describing the steady-state crystallization scenario is found with allowance for a non-linear liquidus equation. The model under consideration takes into account the presence of two phase transition layers, namely, the primary and cotectic mushy regions. We demonstrate that the phase diagram nonlinearity leads to substantial changes of analytical solutions.

1. Introduction

Solidification processes of binary and multicomponent melts frequently occur in the presence of a phase transition layer, which divides purely solid and liquid phases. This layer arising as a result of thermal or constitutional supercooling ahead of the growing solid/liquid interface is called a mushy layer [1–4]. This supercooled layer is filled with the evolving solid phase elements in the form of dendrite-like structures and/or nucleating and growing solid particles [5–18]. If the latent heat of solidification releasing as a result of solid phase evolution completely compensates the mushy layer supercooling, such a two-phase layer is called quasiequilibrium. If the latent heat compensates the system supercooling in part, crystallization process evolves in non-equilibrium manner. Mathematical models of these processes and their analytical solutions in binary melts and solutions were considered in some detail in previous studies for a linear form of the phase diagram (quasiequilibrium [19–27] and non-equilibrium [28–30] theories).

If the solidifying system represents a multicomponent melt, the situation changes rather drastically. So, in the case of a ternary system, two mushy layers appear ahead of the solid phase (primary and cotectic mushy layers). A mathematical model of unidirectional crystallization process of a ternary system with a linear phase diagram was developed by Anderson [31] on the basis of experimental data [32]. Exact analytical solutions of this model were determined for the steady-state and self-similar crystallization conditions in [33–35]. Experimental and theoretical investigations demonstrate that the phase diagram nonlinearity substantially changes the process parameters and characteristics [36–38]. So, for example, nonlinearity in the phase diagram of binary systems increases the mushy layer thikness more than twice [37]. The present study is devoted to the question of how the nonlinear phase diagram influences the physical and process parameters of ternary melt solidification with the primary and cotectic mushy layers.


Content from this work may be used under the terms of the Creative Commons Attribution 3.0 licence. Any further distribution of this work must maintain attribution to the author(s) and the title of the work, journal citation and DOI.
Published under licence by IOP Publishing Ltd

2. The model of directional solidification of ternary systems

Let us consider the process of directional solidification of a ternary system along the spatial axis z (see Figure 1) and designate the concertrations of two substances dissolved in a solvent A as B and C ($A + B + C = 1$). As the main material undergoes a phase transition in a layer, which does not coincide with a phase transition region of the second component, two phase transition zones, primary and cotectic, are capable to appear in the solidification process. We denote their lengths as σ_P and σ_C (here subscripts P and C correspond to the primary and cotectic layers). Taking into account that the system phase diagram was discussed in details in refs. [34,35] we will not dwell on this point here and refer the reader to these original publications instead. An important point is that the temperature relaxation time $\tau_T \sim l^2/\kappa$ is much smaller than a characteristic relaxation time of the concentration fields $\tau_B \sim l^2/D_B$ and $\tau_C \sim l^2/D_C$, i.e. $\tau_T \ll \tau_C$ and $\tau_T \ll \tau_B$ (l - is a characteristic length scale, κ is the thermal diffusivity, D_B and D_C are the diffusion coefficients of B and C components). These estimates for the relaxation times show that the temperature derivatives with respect to time τ are much smaller than the other terms of corresponding model equations. With this in mind, we write down a mathematical model of the process based on the previous papers [33–35].

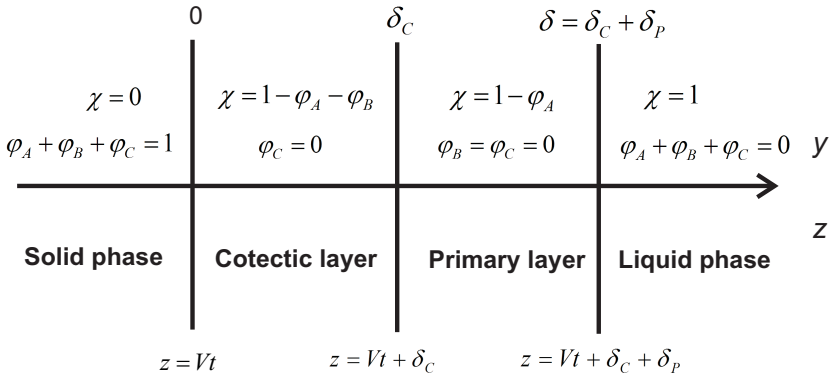

Figure 1. A scheme of the unidirectional crystallization process of a three-component system with two phase transition layers.

The impurity concentrations B_∞ and C_∞ in the liquid phase (melt) and the temperature gradient G_L will be regarded as known

$$B \to B_\infty,\ C \to C_\infty,\ z \to \infty, \tag{1}$$

$$\frac{\partial T}{\partial z} = G_L,\ z > Vt + \delta = Vt + \delta_C + \delta_P, \tag{2}$$

where T is the temperature, and V is the constant solidification rate. In addition, the following diffusion equations in liquid hold true

$$\frac{\partial B}{\partial t} = D_B \frac{\partial^2 B}{\partial z^2},\ \frac{\partial C}{\partial t} = D_C \frac{\partial^2 C}{\partial z^2},\ z > Vt + \delta. \tag{3}$$

The boundary conditions at the primary two phase layer - melt interface represent the heat and mass balance and the continuity conditions written out in the form of

$$L_V V\,[\varphi_A]^+_- = \left[\bar{k}\frac{\partial T}{\partial z}\right]^+_-,\ [T]^+_- = [B]^+_- = [C]^+_- = 0,\ z = Vt + \delta, \tag{4}$$

$$BV\left[\varphi_A\right]_-^+ = D_B\left[\chi\frac{\partial B}{\partial z}\right]_-^+,\ CV\left[\varphi_A\right]_-^+ = D_C\left[\chi\frac{\partial C}{\partial z}\right]_-^+,\ z = Vt+\delta. \tag{5}$$

Here L_V is the latent heat of solidification, $\bar{k} = k_L\chi + k_S\left(1-\chi\right)$, k_L and k_S are the thermal conductivity coefficients in the melt and solid phases, χ is the liquid phase fraction, φ_A is the solid phase fraction of component A. The symbol $[.]_-^+$ denotes a jump of the corresponding value at the boundary.

The heat and mass transfer equations in the primary two-phase layer, where the phase transition undergoes the component A ($\chi = 1-\varphi_A$), can be expressed as

$$\frac{\partial}{\partial z}\left(\bar{k}\frac{dT}{dz}\right) + L_V\frac{\partial\varphi_A}{\partial t} = 0,\ T = T_M + m_B B + m_C C + n_C C^2,\ Vt+\delta_C < z < Vt+\delta, \tag{6}$$

$$D_B\frac{\partial}{\partial z}\left(\chi\frac{\partial B}{\partial z}\right) - \frac{\partial}{\partial t}\left(\chi^B\right) = 0,\ D_C\frac{\partial}{\partial z}\left(\chi\frac{\partial C}{\partial z}\right) - \frac{\partial}{\partial t}\left(\chi^C\right) = 0,\ Vt+\delta_C < z < Vt+\delta. \tag{7}$$

Here T_M is the phase transition temperature of the pure substance, m_B and m_C are the liquidus slope coefficients.

Let us write down the boundary conditions at the second phase interface between the cotectic and primary layers. These conditions, reflecting the heat and mass balance as well as the continuity of temperature and concentration fields, read [31, 33–35]

$$L_V V\left[\varphi_A+\varphi_B\right]_-^+ = \left[\bar{k}\frac{\partial T}{\partial z}\right]_-^+,\ \left[T\right]_-^+ = \left[B\right]_-^+ = \left[C\right]_-^+ = 0, \tag{8}$$

$$B = B^C\left(T\right),\ C = C^C\left(T\right),\ z = Vt+\delta_C, \tag{9}$$

$$V\{B\left[\varphi_A\right]_-^+ + (B-1)\left[\varphi_B\right]_-^+\} = D_B\left[\chi\frac{\partial B}{\partial z}\right]_-^+,\ VC\left[\varphi_A+\varphi_B\right]_-^+ = D_C\left[\chi\frac{\partial C}{\partial z}\right]_-^+,\ z = Vt+\delta_C, \tag{10}$$

where φ_B indicates the solid phase fraction of component B.

Further, the heat and mass transfer equations in the cotectic mushy layer, where the phase transition undergo two components A and B ($\chi = 1-\varphi_A-\varphi_B$), take the form

$$\frac{\partial}{\partial z}\left(\bar{k}\frac{\partial T}{\partial z}\right) + L_V\frac{\partial\left(\varphi_A+\varphi_B\right)}{\partial t} = 0,\ Vt < z < Vt+\delta_C, \tag{11}$$

$$B = B^C\left(T\right) = \frac{T_E + m_B^C B_E - T}{m_B^C},\ T = T_E^{AB} - m_C^C C + n_C^C C^2,\ Vt < z < Vt+\delta_C, \tag{12}$$

$$D_B\frac{\partial}{\partial z}\left(\chi\frac{\partial B}{\partial z}\right) - \frac{\partial}{\partial t}\left(\chi^B+\varphi_B\right) = 0,\ D_C\frac{\partial}{\partial z}\left(\chi\frac{\partial C}{\partial z}\right) - \frac{\partial}{\partial t}\left(\chi^C\right) = 0,\ Vt < z < Vt+\delta_C. \tag{13}$$

Here T_E, B_E and C_E are the known values of temperature and impurity concentrations at the eutectic point of ternary system and T_E^{AB} is the eutectic temperature of binary system. The boundary conditions at the interface between the solid phase and cotectic layer are

$$L_V V\left[\varphi_A+\varphi_B+\varphi_C\right]_-^+=\left[\bar{k}\frac{\partial T}{\partial z}\right]_-^+,\ z=Vt, \tag{14}$$

$$V\{B\left[\varphi_A\right]_-^+ +(B-1)\left[\varphi_B\right]_-^+ +B\left[\varphi_C\right]_-^+\}=D_B\left[\chi\frac{\partial B}{\partial z}\right]_-^+,\ z=Vt, \tag{15}$$

$$V\{C\left[\varphi_A\right]_-^+ +C\left[\varphi_B\right]_-^+ +(C-1)\left[\varphi_C\right]_-^+\}=D_C\left[\chi\frac{\partial C}{\partial z}\right]_-^+,\ z=Vt. \tag{16}$$

In the solid phase, we have a constant temperature gradient G_S, i.e.

$$\frac{\partial T}{\partial z}=G_S,\ z<Vt. \tag{17}$$

The model (1)-(17) represents a closed system of equations and boundary conditions and enables us to find the model solution, which describes the steady-state ternary melt crystallization.

3. Analytical solution of nonlinear model

Let us introduce the coordinate system which moves with the constant velocity V. The crystallization process is established in the new coordinate system where all unknown functions are independent of time. One can easily show that the diffusion equations (3) supplemented by the boundary conditions (1), have the following integrals

$$B\left(y\right)=B_\infty+B_1\exp\left(\frac{-Vy}{D_B}\right),\ C\left(y\right)=C_\infty+C_1\exp\left(\frac{-Vy}{D_C}\right),\ y>\delta=\delta_C+\delta_P, \tag{18}$$

where B_1 and C_1 are the constants of integration. Futher, we find the temperature and concentration derivatives performing the integration of heat and mass transfer equations (6) and (7) in the primary two-phase layer

$$\frac{dT}{dy}=\frac{\left(L_V V\varphi_A+A_1\right)}{\bar{k_P}\left(\varphi_A\right)},\ \bar{k_P}\left(\varphi_A\right)=k_L\left(1-\varphi_A\right)+k_S\varphi_A,\ \delta_C<y<\delta, \tag{19}$$

$$\frac{dB}{dy}=\frac{A_2-BV\left(1-\varphi_A\right)}{D_B\left(1-\varphi_A\right)},\ \frac{dC}{dy}=\frac{A_3-CV\left(1-\varphi_A\right)}{D_C\left(1-\varphi_A\right)},\ \delta_C<y<\delta, \tag{20}$$

where $A_1=\bar{k_P}\left(\varphi_{\bar{A}PL}\right)G_{PL}-VL_V\varphi_{\bar{A}PL}$, A_2 and A_3 are the constants of integration, G_{PL} and $\varphi_{\bar{A}PL}$ are the temperature gradient and solid phase fraction at $y=\delta$. These unknowns will be found below. Furher, combining expressions (19), (20) and the liquidus equation (6), we determine the relationship between concentrations B and C in the primary two-phase region as

$$B\left(\varphi_A\right)=g\left(\varphi_A\right)-\frac{D_B m_C}{D_C m_B}C\left(\varphi_A\right)+\frac{2A_3 n_C D_B}{Vm_B D_C\left(1-\varphi_A\right)}C\left(\varphi_A\right)-\frac{2n_C D_B}{m_B D_C}C^2\left(\varphi_A\right),\ \delta_C<y<\delta,$$

$$g\left(\varphi_A\right)=\frac{D_B}{Vm_B}\left[\frac{m_B A_2}{D_B\left(1-\varphi_A\right)}+\frac{m_C A_3}{D_C\left(1-\varphi_A\right)}\right.$$
$$\left.-\frac{\left(L_V V\left(\varphi_A-\varphi_{\bar{A}_{PL}}\right)+\bar{k_P}\left(\varphi_{\bar{A}_{PL}}\right)G_{PL}\right)}{\bar{k_P}\left(\varphi_A\right)}\right]. \tag{21}$$

Now we define $\frac{dB}{dC}$ in the primary mushy zone from expression (20)

$$\frac{dB}{dC} = \frac{(A_2 - VB(1-\varphi_A))D_C}{(A_3 - VC(1-\varphi_A))D_B}. \tag{22}$$

Next, we consider the case $D_B \neq D_C$ and substitute dB from (21) into (22). As a result, we obtain the expression

$$\frac{dC}{d\varphi_A} = \Bigg[\frac{-2A_3 D_B n_C}{Vm_B(1-\varphi_A)D_C g'(\varphi_A)} + \frac{m_C D_B}{m_B D_C g'(\varphi_A)} + \frac{4n_C D_B C}{m_B D_C g'(\varphi_A)}$$

$$+\frac{D_C\left(A_2 - V(1-\varphi_A)\left[g(\varphi_A) + C\left(\frac{2A_3 n_C D_B}{Vm_B D_C(1-\varphi_A)} - \frac{m_C D_B}{m_B D_C}\right) - \frac{2n_C D_B}{m_B D_C}C^2\right]\right)}{D_B(A_3 - VC(1-\varphi_A))g'(\varphi_A)}\Bigg]^{-1}. \tag{23}$$

The boundary condition for this equation can be obtained from expression (10). Combining formulas (20) and (23), we obtain

$$y(\varphi_A) = \delta_C + \int\limits_{\varphi^+_{A_{CP}}}^{\varphi_A} \frac{dC}{d\varphi_A}\frac{D_C(1-\varphi_A)}{A_3 - VC(1-\varphi_A)}d\varphi_A, \tag{24}$$

$$\delta = \delta_C + \delta_P = \delta_C + \int\limits_{\varphi^+_{A_{CP}}}^{\varphi^-_{A_{PL}}} \frac{dC}{d\varphi_A}\frac{D_C(1-\varphi_A)}{A_3 - VC(1-\varphi_A)}d\varphi_A. \tag{25}$$

Expressions (21)-(25) represent the parametric solution in the primary mushy layer (with parameter φ_A (or $\chi = 1-\varphi_A$)).

Substituting these solutions into the boundary conditions (4), (5) we get

$$G_L = \frac{-m_B V B_1}{D_B}\exp\left(-\frac{V\delta}{D_B}\right) - \frac{m_C V C_1}{D_C}\exp\left(-\frac{V\delta}{D_C}\right)$$

$$+2n_C\left(C_\infty + C_1\exp\left(-\frac{V\delta}{D_C}\right)\right)\left(\frac{VC_1}{D_C}\exp\left(-\frac{V\delta}{D_C}\right)\right), \tag{26}$$

$$G_{PL} = \frac{k_L G_L + L_V V\varphi^-_{APL}}{k^-_P\left(\varphi^-_{APL}\right)},\ A_2 = VB_\infty,\ A_3 = VC_\infty, \tag{27}$$

$$B_1 = \exp\left(\frac{V\delta}{D_B}\right)\Bigg[g\left(\varphi^-_{A_{PL}}\right) - B_\infty + \left(\frac{2A_3 n_C D_B}{Vm_B D_C\left(1-\varphi^-_{A_{PL}}\right)} - \frac{m_C D_B}{m_B D_C}\right)$$

$$\times\left(C_\infty + C_1\exp\left(-\frac{V\delta}{D_C}\right)\right) - \frac{2n_C D_B}{m_B D_C}\left(C_\infty + C_1\exp\left(-\frac{V\delta}{D_C}\right)\right)^2\Bigg], \tag{28}$$

$$C_\infty + C_1\exp\left(-\frac{V\delta}{D_C}\right) = C\left(\varphi^-_{APL}\right). \tag{29}$$

Next let us solve the problem in the cotectic zone. Integrating equations (11) and (13), we have

$$D_B\chi\frac{dB}{dy}+VB\chi+V\varphi_B=A_6,\ D_C\chi\frac{dC}{dy}+VC\chi=A_7, \tag{30}$$

$$\frac{dT}{dy}=\frac{\bar{k_C}\left(\chi_{SC}^{+}\right)G_{SC}-VL_V\left(1-\chi_{SC}^{+}\right)+VL_V\left(1-\chi\right)}{\bar{k_C}\left(\chi\right)}\equiv F_0\left(\chi\right). \tag{31}$$

Differentiating equation (12) one can obtain expressions connecting $\frac{dB}{dy}$, $\frac{dC}{dy}$ and $\frac{dT}{dy}$. Substituting them into (30) and (31), we obtain $\varphi_B\left(\chi\right)$, $\varphi_A\left(\chi\right)$ and $C\left(\chi\right)$

$$\varphi_B\left(\chi\right)=\frac{D_B\chi}{m_B^C V}F_0\left(\chi\right)+\frac{A_6}{V}-\chi B\left(\chi\right),\ \varphi_A\left(\chi\right)=1-\chi-\varphi_B\left(\chi\right), \tag{32}$$

$$C^2\left(\chi\right)\cdot\left(\frac{-2Vn_C^C}{D_C}\right)+C\left(\chi\right)\cdot\left(\frac{Vm_C^C}{D_C}+\frac{2n_C^CA_7}{D_C\chi}\right)-\left(\frac{m_C^CA_7}{D_C\chi}+F_0\left(\chi\right)\right)=0. \tag{33}$$

From (12), we get

$$B\left(\chi\right)=\frac{-n_C^C}{m_B^C}C^2\left(\chi\right)+m_{CB}^CC\left(\chi\right)+B_E+\frac{T_E-T_E^{AB}}{m_B^C}. \tag{34}$$

Note that only one of two solutions of equation (33) lies within the unit interval. Analyzing both solutions, we choose one of them (physically admissible)

$$C\left(\chi\right)=\frac{\frac{Vm_C^C}{D_C}+\frac{2n_C^CA_7}{D_C\chi}-\sqrt{\left(\frac{Vm_C^C}{D_C}+\frac{2n_C^CA_7}{D_C\chi}\right)^2-4\frac{2Vn_C^C}{D_C}\frac{m_C^CA_7}{D_C\chi}-4\frac{2Vn_C^C}{D_C}F_0\left(\chi\right)}}{\frac{4Vn_C^C}{D_C}}. \tag{35}$$

Furthermore, from expression (31), we come to the liquid phase fraction and thickness of the cotectic two-phase layer in the form

$$y\left(\chi\right)=\int\limits_{\chi_{SC}^{+}}^{\chi}\frac{dT}{d\chi}\frac{1}{F_0\left(\chi\right)}d\chi, \tag{36}$$

$$\delta_C=\int\limits_{\chi_{SC}^{+}}^{\chi_{CP}^{-}}\frac{dT}{d\chi}\frac{1}{F_0\left(\chi\right)}d\chi. \tag{37}$$

Substituting these solutions into the boundary conditions (14) - (16) and taking into account the temperature gradient (17), we arrive at the following expressions for constants

$$G_{SC}=\frac{k_SG_S-L_VV\chi_{SC}^{+}}{\bar{k_C}\left(\chi_{SC}^{+}\right)},\ V\left(\varphi_{BSC}^{-}-\varphi_{BSC}^{+}-B_E\chi_{SC}^{+}\right)+V\left(B_E\chi_{SC}^{+}+\varphi_{BSC}^{+}\right)=A_6, \tag{38}$$

$$V\left(\varphi_{CSC}^{-}-\varphi_{CSC}^{+}-C_E\chi_{SC}^{+}\right)+VC_E\chi_{SC}^{+}=A_7, \tag{39}$$

$$A_7=\frac{\left(G_{SC}D_C+2C_E^2Vn_C^C-C_EVm_C^C\right)\chi_{SC}^{+}}{2n_C^CC_E-m_C^C}, \tag{40}$$

where φ^-_{BSC} and φ^+_{BSC} are the solid phase fractions of component B on the left and right sides of the solid phase - cotectic layer boundary, φ^-_{CSC} and φ^+_{CSC} are the similar values for the component C. The boundary conditions (9) - (10) give

$$V = \frac{k_S G_S - k_L G_L}{L_V},\ A_6 = A_2 = VB_\infty, \tag{41}$$

$$A_7 = A_3 = VC_\infty, \tag{42}$$

$$C_{CP} = \frac{\frac{Vm^C_C}{D_C} + \frac{2n^C_C A_7}{D_C \chi^-_{CP}} - \sqrt{\left(\frac{Vm^C_C}{D_C} + \frac{2n^C_C A_7}{D_C \chi^-_{CP}}\right)^2 - 4\frac{2Vn^C_C}{D_C}\frac{m^C_C A_7}{D_C \chi^-_{CP}} - 4\frac{2Vn^C_C}{D_C}F_0\left(\chi^-_{CP}\right)}}{\frac{4Vn^C_C}{D_C}}, \tag{43}$$

$$B_\infty - \left(1 - \varphi^+_{A_{CP}}\right)\left[B^* - \frac{n^C_C}{m^C_B}C^2_{CP} + m^C_{CB}C_{CP}\right]$$

$$= m^C_{CB}D_{BC}\left(C_\infty - C_{CP}\left(1 - \varphi^+_{A_{CP}}\right)\right) - 2\frac{n^C_C}{m^C_B}D_{BC}\left(C_\infty C_{CP} - C^2_{CP}\left(1 - \varphi^+_{A_{CP}}\right)\right), \tag{44}$$

$$C^2_{CP}\left(\frac{-2n_C D_B}{m_B D_C} + \frac{n^C_C}{m^C_B}\right)$$

$$+C_{CP}\left(\frac{2C_\infty n_C D_B}{m_B D_C\left(1 - \varphi^+_{A_{CP}}\right)} - \frac{m_C D_B}{m_B D_C} - m^C_{CB}\right) + g\left(\varphi^+_{A_{CP}}\right) - B^* = 0, \tag{45}$$

where $D_{BC} = \frac{D_B}{D_C}$, $m^C_{CB} = \frac{m^C_C}{m^C_B}$, $B^* = B_E + \frac{T_E - T^{AB}_E}{m^C_B}$. Now combining (38), (40) and (42), we obtain the following expressions

$$a_2\left(\chi^+_{SC}\right)^2 + a_1\left(\chi^+_{SC}\right) + a_0 = 0, \tag{46}$$

$$\chi^+_{SC} = \frac{-a_1 \pm \sqrt{a_1^2 - 4a_2 a_0}}{2a_2}, \tag{47}$$

where

$$a_2 = -VL_V D_C + 2C^2_E Vn^C_C k_l - 2C^2_E Vn^C_C k_S - C_E Vm^C_C k_l + C_E Vm^C_C k_S,$$

$$a_1 = -Vk_l C_\infty\left(2n^C_C C_E - m^C_C\right) + C_\infty k_S V\left(2C_E n^C_C - m^C_C\right) + k_S G_S D_C + 2C^2_E Vn^C_C k_S - VC_E m^C_C k_S,$$

$$a_0 = -C_\infty k_S V\left(2C_E n^C_C - m^C_C\right).$$

Now from (38), (39) and (41), (42), one can get

$$\varphi^-_{B_{SC}} = B_\infty, \tag{48}$$

$$\varphi^{-}_{C_{SC}} = C_{\infty}, \tag{49}$$

$$\varphi^{+}_{C_{SC}} = 0. \tag{50}$$

Furthermore, we find $\varphi^{+}_{A_{CP}}$ and C_{CP} from expressions (44) and (45). Then we find χ^{-}_{CP} from (43) with allowance for C_{CP}. In addition, one can solve the differential equation (43) because $C_{CP} = C\left(\varphi^{+}_{A_{CP}}\right)$ is known. Next, combining expressions (26), (28), and (29), we obtain equations determining $\varphi^{-}_{A_{PL}}$, C_1 and B_1. The boundary values on the right side of interface between the solid and cotectic phases can be found from distributions (32) as $\varphi^{+}_{ASC} = \varphi_A\left(\chi^{+}_{SC}\right)$ and $\varphi^{+}_{BSC} = \varphi_B\left(\chi^{+}_{SC}\right)$. Furthermore, distribution (32) also determines the boundary values of solid phase fractions φ^{-}_{ACP} and φ^{-}_{BCP} of components A and B on the left side of interface between the primary and cotectic layers as $\varphi^{-}_{ACP} = \varphi_A\left(\chi^{-}_{CP}\right)$ and $\varphi^{-}_{BCP} = \varphi_B\left(\chi^{-}_{CP}\right)$.

4. Interdendritic spacing

Let us now calculate the primary interdendritic spacing on the basis of known impurity concentration as a function of spatial coordinate. In order to find the analytical dependence for interdendritic spacing λ, we use the previous theory [39]

$$\lambda = \sqrt{\frac{2\pi\rho}{0.86\frac{\partial(\varphi_A+\varphi_B)}{\partial y}}}, \tag{51}$$

where ρ is the radius of curvature corresponding to a stable mode of dendritic growth. The solvability theory [11, 40, 41] gives

$$\frac{2d_0D_T}{\rho^2V_d} = \sigma_0\beta^{7/4}\left[\frac{1}{\left(1+a_1\sqrt{\beta}P_g\right)^2} + \frac{1}{\left(1+a_2\sqrt{\beta}P_g\frac{D_T}{D_C}\right)^2}\frac{2m^C_C C_i\left(1-k_0\right)D_T}{\frac{Q}{c_P}D_C}\right], \tag{52}$$

where

$$C_i = \frac{C_{CP}}{1-(1-k_0)\exp\left(P_g\frac{D_T}{D_C}\right)P_g\frac{D_T}{D_C}I_C\left(\infty\right)}, \tag{53}$$

$$I_C\left(\eta\right) = \int_1^{\eta}\exp\left[-P_g\frac{D_T}{D_C}h\right]\frac{dh}{\sqrt{h}}, \tag{54}$$

$a_2 = \sqrt{2}a_1 \approx 0.505\sqrt{\sigma_0}$, σ_0 is a fitting parameter, d_0 is the capillary length,V_d is the dendrite tip velocity, β is the anisotropic parameter, m^C_C is the liquidus slope, C_i is the concentration of impurity at the dendritic surface, k_0 is the equilibrium partition coefficient, Q is the latent heat per unit volume of the solid phase, c_P is the heat capacity, D_T is the thermal diffusivity, D_C is the solute diffusivity, and P_g is the growth Peclet number. Taking into account the theory under consideration one can calculate the explicit function $\lambda\left(P_g\right)$ on the basis of expressions (51)-(54).

5. Discussion

A new analytical method for solving the problem of heat and mass transfer in a ternary system is developed in this study. The distriburions of impurity concentration as well as of the solid and liquid fractions in the phase transition layer are obtained. The effect of quadratic term in the liquidus equation is studied as well.

Figure 2 shows the effect of deviation of the liquidus equation (coefficient n) from its linear dependence. So, its small deviations (at a fixed impurity concentration) are capable to change the reduced temperature several degrees. It should be noted that such variations often occur in practice. Fig. 2 shows that the temperature decreases with decreasing n and vice versa.

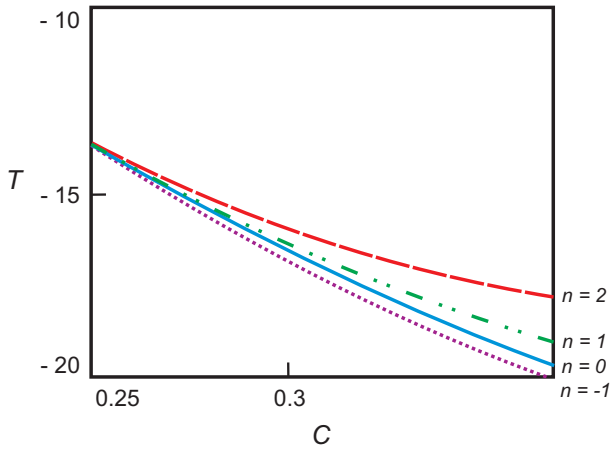

Figure 2. The influence of coefficient n on the deviation of liquidus equation from a linear function (temperature T is measured in Celcius).

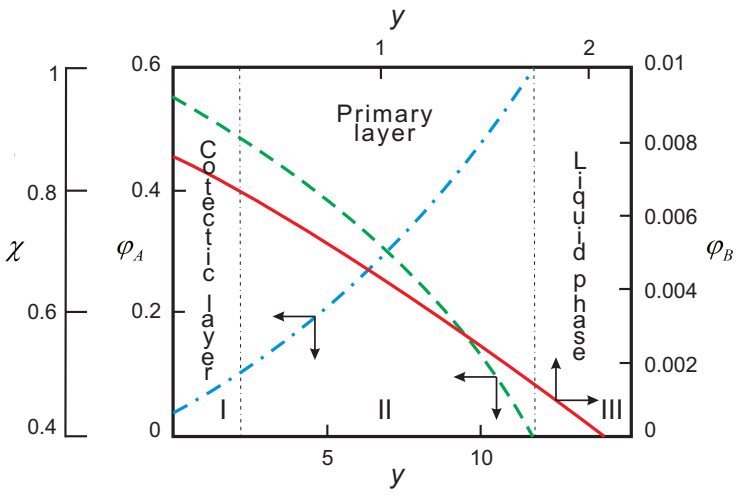

Figure 3. The solid fractions (solid and dashed lines), liquid fraction (dash-dotted line) as functions of the spatial coordinate. The cotectic, primary and liquid layers respectively correspond to regions I, II and III. The physical parameters are given in table 1 (y is measured in cantimeters).

Figure 3 illustrates the solid and liquid phase distributions in the phase transition layer

consisting of the primary and cotectic regions. The solid fraction φ_A of component A, which undergoes the phase transformation in regions I and II, decreases monotonically in the phase transition layer. In contrast, the solid fraction φ_B of component B, which undergoes the phase transition in region I, decreases in the cotectic layer only. The cotectic layer length (region I) therewith is lesser than the main layer (region II) of the phase transition. Accordingly to these dependencies, the liquid phase fraction χ increases monotonically in the total phase transformation domain (regions I and II). In addition, it is defined by the solid fractions φ_A and φ_B in region I, whereas it is described by fraction φ_A in region II. For this reason, the distribution $\chi(x)$ also has an inflection point in the primary layer as well as the solid fraction $\varphi_A(x)$. Our calculations show that the solid and liquid phase fractions at the boundaries between regions I and II, and II and III are continuous.

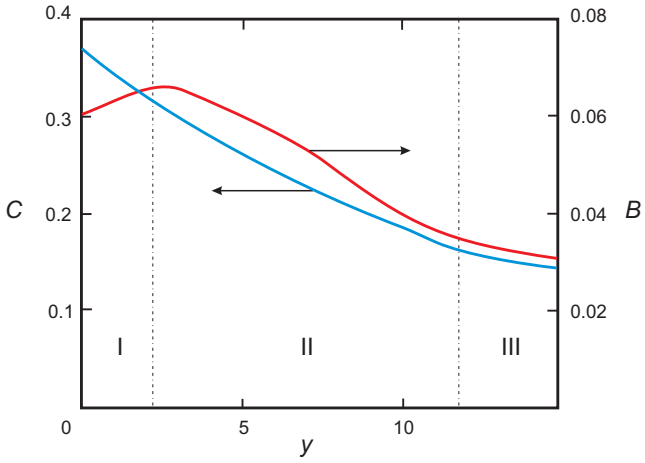

Figure 4. The impurity concentrations C and B as functions of the spatial coordinate $y = z - Vt$. All physical parameters correspond to Figure 2, $\delta_C = 2.168$ cm, $\delta = 11.803$ cm (y is measured in cantimeters).

Figure 4 demonstrates the distributions of impurity concentrations in the entire region of phase transition. The main impurity component, having a concentration $C(x)$, decreases monotonically in regions I and II due to the effect of impurity displacement by the growing solid phase. In contrast to this dependence, having a traditional behavior, the impurity concentration of the second component $B(x)$ increases in the cotectic layer, crosses the boundary between regions I and II, reaches a maximum in the primary mushy zone and then decreases to the initial concentration B_∞. This, at first sight, unusual behavior of the impurity concentration $B(x)$, occurs due to the fact that component B undergoes the phase transition in region I (this leads to a decreased concentration near the solid phase - cotectic layer boundary). Note that a similar behavior of the impurity concentration was obtained in the analysis of self-similar crystallization in references [13, 14, 40, 42, 43]. However, in these studies, the maximum point was found on the boundary of regions I and II. The reason explaining the maximum point displacement into region II lies in the fact that previous studies (see references [13, 14, 40, 42, 43]) have been carried out on the basis of approximate Sheil equations governing the impurity concentrations (equations without diffusion terms). Therefore, in a real ternary system, the maximum point displacement into the primary layer occurs due to the influence of diffusion transport of component $B(x)$.

It should be noted that the influence of coefficient n of the liquidus equation is seen in Figures 3 and 4. All dependencies have the same behavior, however the mushy region length increases significantly in comparison with the linear liquidus line equation.

Figure 5 shows the interdendritic lengh λ as a function of the growth Peclet number P_g. Note that the interdendritic spacing decreases with increasing P_g. This behavior is in consistent with known experimental data [44, 45] and the previously developed theory [46].

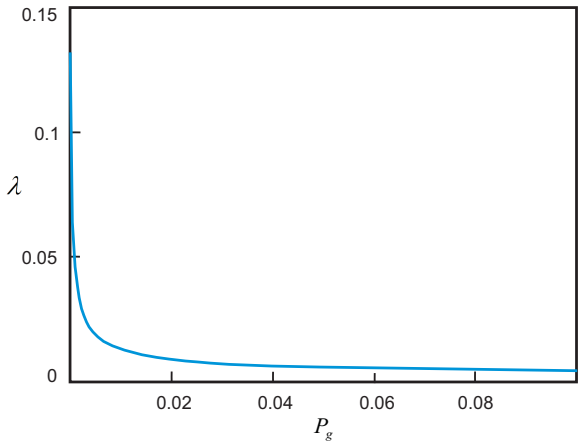

Figure 5. The interdendritic spacing λ (measured in cantimeters) as a function of the growth Peclet number P_g (thermophysical parameters are listed in Table 1).

Table 1. The physical parameters of three-component system $H_2O - KNO_3 - NaNO_3$ (B and C designate $NaNO_3$ and KNO_3).

B_E	0.06
C_E	0.37
B_E^{AB}	0.10
B_∞	0.035
C_∞	0.152
T_E (^{0}C)	-19
T_E^{AB} (^{0}C)	-5
T_M (^{0}C)	0
κ (cm^{2}s^{-1})	$1.1 \cdot 10^{-3}$
D_C (cm^{2}s^{-1})	$4.94 \cdot 10^{-6}$
D_B (cm^{2}s^{-1})	$4.94 \cdot 10^{-6}$
L_V/k_S (s^{0}C cm^{-2})	$1.52 \cdot 10^5$
k_L/k_S	0.25
k_S	$5.3 \cdot 10^{-3}$
G_S (^{0}C cm^{-1})	1
k_0	0
σ_0	2.1
β	0.195

The main result of this paper lies in the fact that even small deviations of the liquidus equation from a linear dependence can be responsible for significant changes of other parameters governing the ternary melt solidification process.

This work was partially supported by the Russian Foundation for Basic Research (grant no. 16-08-00932).

6. References

[1] Hills R N, Loper D E and Roberts P H 1983 *Q. J. Appl. Math.* **36** 505–539
[2] Fowler A C 1985 *IMA J. Appl. Math.* **35** 159–174
[3] Buyevich Yu A, Alexandrov D V and Mansurov V V 2001 *Macrokinetics of Crystallization* (New York: Begell House)
[4] Alexandrova I V, Alexandrov D V, Aseev D L and Bulitcheva S V 2009 *Acta Physica Polonica A* **115** 791–794
[5] Mullin J W 1972 *Crystallization* (London: Butterworth)
[6] Huppert H 1990 *J. Fluid Mech.* **212** 209-240
[7] Pelcé P 1988 *Dynamics of Curved Fronts* (Boston: Academic Press)
[8] Herlach D M 2008 *Phase Transformations in Multicomponent Melts* (Weinheim: Wiley-VCH)
[9] Herlach D M 2015 *Crystals* **5** 355–375
[10] Alexandrov D V, Galenko P K and Herlach D M 2010 *J. Crystal Growth* **312** 2122–2127
[11] Alexandrov D V and Galenko P K 2013 *Phys. Rev. E* **87** 062403
[12] Alexandrov D V and Malygin A P 2013 *J. Phys. A: Math. Theor.* **46** 455101
[13] Alexandrov D V and Nizovtseva I G 2014 *Proc. R. Soc. A* **470** 20130647
[14] Alexandrov D V and Malygin A P 2014 *Modelling Simul. Mater. Sci. Eng.* **22** 015003
[15] Alexandrov D V 2014 *Phys. Lett. A* **378** 1501–1504
[16] Alexandrov D V 2014 *J. Phys. A: Math. Theor.* **47** 125102
[17] Alexandrov D V 2014 *Phil. Mag. Lett.* **94** 786–793
[18] Shneidman V A 2013 *Phys. Rev. E* **88** 010401
[19] Worster M G 1986 *J. Fluid Mech.* **167** 481–501
[20] Alexandrov D V and Aseev D L 2005 *J. Fluid Mech.* **527** 57–66
[21] Alexandrov D V and Aseev D L 2006 *Comput. Mater. Sci.* **37** 1–6
[22] Aseev D L and Alexandrov D V 2006 *Acta Mater.* **54** 2401–2406
[23] Alexandrov D V, Aseev D L, Nizovtseva I G, Huang H-N and Lee D 2007 *Int. J. Heat Mass Trans.* **51** 5204–5208
[24] Alexandrov D V, Nizovtseva I G, Malygin A P, Huang,H-N and Lee D 2008 *J. Phys.: Condens. Matter* **20** 114105
[25] Alexandrov D V and Nizovtseva I G 2008 *Int. J. Heat Mass Trans.* **51** 5204–5208
[26] Alexandrov D V and Malygin A P 2011 *Int. J. Heat Mass Trans.* **54** 1144–1149
[27] Alexandrov D V and Malygin A P 2012 *Int. J. Heat Mass Trans.* **55** 3196–3204
[28] Aseev D L and Alexandrov D V 2006 *Int. J. Heat Mass Trans.* **49** 4903–4909
[29] Aseev D L and Alexandrov D V 2006 *Doklady Physics* **51** 291–295
[30] Alexandrov D V and Malygin A P 2011 *Phys. Earth Planet. Int.* **189** 134–141
[31] Anderson D M 2003 *J. Fluid Mech.* **483** 165–197
[32] Aitta A, Huppert H E and Worster M G 2001 *J. Fluid Mech.* **432** 201–217
[33] Alexandrov D V and Malygin A P 2012 *Int. J. Heat Mass Trans.* **55** 3755–3762
[34] Alexandrov D V and Ivanov A A 2009 *Int. J. Heat Mass Trans.* **52** 4807–4811
[35] Alexandrov D V and Ivanov A A 2009 *J. Exper. Theor. Phys.* **108** 821–829
[36] Jordan A S 1971 *Metall. Trans.* **2** 1965–1970
[37] Alexandrov D V, Rakhmatullina I V and Malygin A P 2010 *Russian Metallurgy (Metally)* **8** 745–750
[38] Herlach D M and Matson D M 2012 *Solidification of Containerless Undercooled Melts* (Weinheim: WileyVCH)
[39] Deguen R, Alboussiére A and Brito D 2007 *Phys. Earth Planet. Inter.* **164** 36-49
[40] Alexandrov D V and Galenko P K 2014 *Physics-Uspekhi* **57** 771-786
[41] Alexandrov D V and Galenko P K 2015 *Phys. Chem. Chem. Phys.* **17** 19149-19161
[42] Alexandrov D V 2003 *Physics-Doklady* **48** 481-486
[43] Gao J, Han M, Kao A, Pericleous K, Alexandrov D V and Galenko P K 2016 *Acta Materialia* **103** 184-191
[44] Somboonsuk K, Mason J T and Trivedi R 1984 *Metall. Trans. A* **15A** 967-975
[45] Trivedi R 1984 *Metall. Trans. A* **15A** 977-982
[46] Alexandrov D V and Britousova A V 2015 *AIP Conference Proceedings* **1648** 850101

Acknowledgments

This work was supported by the Russian Foundation for Basic Research (grant no. 16-08-00932) and the Ministry of Education and Science of the Russian Federation (project no. 1.9527.2017).